

Xinfeng Capsule Inhibits Pyroptosis and Ameliorates Myocardial Injury in Rats with Adjuvant Arthritis via the GAS5/miR-21/TLR4 Axis

Wanlan Fu¹, Yunxiang Cao², Jian Liu², Chuanbing Huang², Kaiyan Shu¹, Nanfei Zhu¹

¹First Clinical Medical College, Anhui University of Chinese Medicine, Hefei, Anhui, 230012, People's Republic of China; ²Department of Rheumatology, First Affiliated Hospital of Anhui University of Chinese Medicine, Hefei, Anhui, 230031, People's Republic of China

Correspondence: Yunxiang Cao, Department of Rheumatology, First Affiliated Hospital of Anhui University of Chinese Medicine, 117 Meishan Road, Shushan District, Hefei, Anhui, 230031, People's Republic of China, Tel +86-13514984395; +0551-62838591, Email cyx800805@163.com

Purpose: This study probed the mechanism of action of Xinfeng Capsule (XFC) in myocardial injury in rats with adjuvant arthritis (AA) via the growth arrest-specific transcript 5 (GAS5)/microRNA-21 (miR-21)/Toll-like receptor 4 (TLR4) axis.

Methods: Rats were injected with Freund's complete adjuvant to establish a rat model of AA. Then, some modeled rats were given normal saline or drugs only, and some modeled rats were injected with adeno-associated viruses or necrosulfonamide (NSA; a pyroptosis inhibitor) before drug administration. Toe swelling and arthritis index (AI) were calculated. Pathological and morphological changes in synovial and myocardial tissues were analyzed with hematoxylin-eosin staining, and pyroptotic vesicles and the ultrastructural changes of myocardial tissues were observed with transmission electron microscopy. The serum levels of interleukin (IL)-1 β , IL-18, IL-6, and tumor necrosis factor (TNF)- α were detected, and lactate dehydrogenase (LDH) release was measured in myocardial tissues, accompanied by the examination of GAS5, miR-21, TLR4, nuclear factor- κ B (NF- κ B) p65, nucleotide-binding oligomerization domain-like receptor protein 3 (NLRP3), Caspase-1, and Gasdermin D (GSDMD) expression in myocardial tissues.

Results: After AA modeling, rats presented with significantly increased toe swelling and AI scores, synovial and myocardial tissue damage, elevated pyroptotic vesicles, and markedly enhanced serum levels of IL-1 β , IL-18, IL-6, and TNF- α , accompanied by significantly diminished GAS5 expression, substantially augmented miR-21, TLR4, NF- κ B p65, NLRP3, Caspase-1, and GSDMD expression, greatly increased LDH release in myocardial tissues. XFC treatment significantly declined toe swelling, AI scores, synovial and myocardial tissue damage, and the serum levels of IL-1 β , IL-18, IL-6, and TNF- α in AA rats. Additionally, XFC treatment markedly elevated GAS5 expression and substantially lowered LDH release and miR-21, TLR4, NF- κ B p65, NLRP3, Caspase-1, and GSDMD expression in myocardial tissues of AA rats. Moreover, the above effects of XFC in AA rats were further promoted by GAS5 overexpression or NSA treatment.

Conclusion: XFC alleviated myocardial injury in AA rats by regulating the GAS5/miR-21/TLR4 axis and inhibiting pyroptosis and pro-inflammatory cytokine secretion.

Keywords: adjuvant arthritis, myocardial injury, GAS5/miR-21/TLR4 axis, pyroptosis, Xinfeng Capsule

Introduction

Rheumatoid arthritis (RA), a chronic systemic inflammatory disease, can lead to joint deformity and dysfunction.¹ RA patients often present with a variety of extra-articular manifestations and comorbidities, including cardiovascular, respiratory, digestive, and cutaneous disorders since this disease involves multiple extra-articular organs, particularly the heart.² Moreover, RA has been demonstrated as an independent risk factor for cardiovascular disease (CVD).³ Reportedly, the mortality rate of CVD is 1.5 times higher in RA patients than in the general population.⁴ In some special cases of RA, extra-articular symptoms may precede the onset of articular symptoms, thereby affecting the regression and

prognosis of RA.^{2,5} Considering the unclear pathogenesis of RA, it is essential for the management of cardiac damage secondary to RA to elucidate the pathogenic mechanisms.

Pyroptosis is a novel type of inflammatory programmed cell death that is mediated by Caspase and gasdermin (GSDM) families.⁶ It has been reported that pyroptosis is involved in the progression of RA.⁷ Pyroptosis-related biological alterations, such as inflammasome formation, activation of Caspases and GSDM proteins, and release of numerous pro-inflammatory cytokines (interleukin [IL]-1 β , IL-18, IL-6, and tumor necrosis factor [TNF]- α), are pivotal triggers of RA.⁸ Similarly, pyroptosis has an important role in the pathogenesis of CVD which is associated with cardiomyocytes, vascular endothelial cells, and macrophages.⁹ Myocardial pyroptosis is widely involved in myocardial injury of various causes and is a key mechanism underlying impaired cardiac function.^{9,10} As a result, pyroptosis inhibition may be a potential strategy to improve cardiac function in RA patients.

Long non-coding RNAs (lncRNAs) are transcripts formed by the transcription of RNA polymerase II longer than 200 nucleotides,¹¹ which modulate several biological processes such as immune response, metabolism, proliferation, differentiation, and apoptosis¹² and also play a unique role in the differentiation and activation of immune cells.¹³ More importantly, lncRNAs can mediate pyroptosis through two mechanisms. Specifically, lncRNAs bind to microRNAs (miRNAs/miRs) as competitive endogenous RNAs (ceRNAs) to affect the expression of messenger RNAs (mRNAs), thus regulating pyroptosis.¹⁴ Additionally, lncRNAs can influence pyroptosis by directly binding to proteins or inhibiting the translation process.¹⁵ These two mechanisms also are implicated in the pathology and physiology of RA and CVD.^{16,17} As a lncRNA, growth arrest-specific transcript 5 (GAS5) has become a hotspot for ceRNA-related research in recent years because of its key role in the regulation of pyroptosis.¹⁸ GAS5 has been revealed as a potential therapeutic target for RA.¹⁹ Furthermore, a prior study exhibited that GAS5 could structurally bind to miR-21 in RAW264.7 macrophages.²⁰ MiR-21, a member of the miRNA family, was found in a previous study to bind to Toll-like receptor 4 (TLR4) in renal tubular epithelial cells induced by ischemia.²¹ Of note, mounting studies indicated that both miR-21 and TLR4 initiate nucleotide-binding oligomerization domain-like receptor protein 3 (NLRP3) inflammasome-mediated pyroptosis through diverse pathways.^{22–24} In addition, a previous study showed that myocardial injury occurred in AA rats, which might be related to the activation of the TLR4/mitogen-activated protein kinase/nuclear factor- κ B (NF- κ B) pathway, the elevated expression of miR-21, and the increased release of pro-inflammatory cytokines.²⁵ Therefore, we hypothesized that GAS5 might act as a ceRNA to bind to miR-21 during the occurrence and development of RA, hence modulating TLR4 expression and affecting myocardial pyroptosis.

Xinfeng Capsule (XFC) is a traditional Chinese medicine (TCM) compound preparation that is developed based on the TCM theory for the treatment of RA.²⁶ Liu et al observed that XFC effectively repressed the immune inflammatory response and improved the cardiac function of RA patients.²⁶ Therefore, this study investigated whether the TCM compound XFC suppressed inflammation and pyroptosis and improved myocardial injury in RA and analyzed the related mechanism of XFC involving the GAS5/miR-21/TLR4 axis.

Materials and Methods

Animals

Forty-two male Sprague-Dawley (SD) rats (specific pathogen-free grade; age: 6–8 weeks; weight: 200–220 g) were purchased from Liaoning Changsheng Biotechnology Co., Ltd. (Liaoning, China; SCXK (Liao) 2020–0001). The rats were acclimatized for 1 week and then reared by groups in the laboratory with a temperature of 20°C–25°C and a relative humidity of 40–70% under natural light cycles. This study was approved by the Animal Ethics Committee of the Anhui University of Chinese Medicine (Approval No. AHUCM-rats-2023033).

Drugs and Reagents

XFC is composed of *Astragalus membranaceus*, Coix seed, Centipede, and *Tripterygium wilfordii*, which was provided by the Preparation Center of the First Affiliated Hospital of Anhui University of Chinese Medicine (Anhui Medicine system Z20050062). Methotrexate (MTX) tablets were purchased from Shanghai Shangyao Xinyi Pharmaceutical Co., Ltd. (Shanghai, China; 036211006). Freund's complete adjuvant (FCA) was acquired from Chondrex (Redmond, Washington,

USA; 7008). Anti- β -actin, anti-TLR4, anti-NF- κ B p65, and anti-GSDMD were bought from Proteintech (Wuhan, China; 81115-1-RR, 19811-1-AP, 10745-1-AP, and 20770-1-AP), while anti-Caspase-1 and anti-NLRP3 were purchased from ZENBID (Chengdu, China; 342947 and 381207). Goat anti-rabbit immunoglobulin G (IgG) and goat anti-mouse IgG, both of which are labeled by horseradish peroxidase, were provided by Zhongshan Jinqiao Biotechnology Co., Ltd. (Beijing, China; ZB-2301 and ZB-2305). Enzyme-linked immunosorbent assay (ELISA) kits of IL-1 β , IL-6, IL-18, and TNF- α were purchased from Shanghai Weiao Biotechnology Co., Ltd. (Shanghai, China; ER20275M, ER20298M, ER20267M, and ER20497M). The hematoxylin-eosin (HE) staining kit was bought from Solarbio (Beijing, China; G1120). The lactate dehydrogenase (LDH) kit was provided by Nanjing Jiancheng Bioengineering Institute (Nanjing, China; A020-1); Adeno-associated viruses (AAV) were designed and synthesized by Limibio (Hefei, China). The pyroptosis inhibitor necrosulfonamide (NSA) was acquired from GLPBIO (Shanghai, China; GC10150).

Instruments

The following instrument was used in this study: a SpectraMax Plus 384 multi-mode microplate reader (Molecular Devices, Sunnyvale, CA, USA), a reverse transcription-quantitative polymerase-chain reaction (RT-qPCR) instrument (Roche, Indianapolis, IN, USA; LightCycler 480), a high-speed tissue grinder (Servicebio, Wuhan, China; KZ-II), an ECLIPSE E100 microscope (NIKON, Tokyo, Japan), a gel imager (Bio-Rad, Hercules, CA, USA; ChemiDoc XRS+ System), an electrophoresis instrument (Bio-Rad; Mini-Protean Tetra System), and a chemiluminescence imaging system (Shenhua Science Technology Co., Ltd. (Hangzhou, China; SH-523)).

AA Modeling, Grouping, and Drug Administration

Forty-two rats were allocated into seven groups (6 rats/group) with the random number table method: normal control (NC), model control (MC), XFC, MTX, XFC + empty adeno-associated viruses (AAVs) (XFC + EV), XFC + AAVs harboring GAS5 overexpression (XFC + GAS5), and XFC + NSA groups. Except for rats in the NC group, rats in other groups were injected intracutaneously with 0.1 mL FCA at the right plantar surface to induce inflammation. On the 10th day after the first FCA injection, rats in the XFC + EV and XFC + GAS5 groups were given a single injection of 100 μ L of empty AAVs (1×10^{13} TU/mL) and 100 μ L of AAVs harboring GAS5 overexpression (1×10^{13} TU/mL), respectively. On the 19th day, rats in the NC and MC groups were given normal saline (1 mL/100 g) once a day, rats in the XFC, XFC + EV, XFC + GAS5, and XFC + NSA groups were given XFC suspensions (0.3 g/mL; 1 mL/100 g) once a day, and rats in the MTX group were given MTX suspensions (0.3 mg/mL; 1 mL/100 g) once a week. In addition, rats in the XFC + NSA group underwent a one-time intraperitoneal injection of NSA (1.65 mg/kg). Rats were administered normal saline or drugs by gavage for 4 weeks.

Assessment of Arthritis Severity

The volume of the hind plantar was measured with the drainage method 1 day before modeling and 2 times a week after modeling to analyze toe swelling. Toe swelling was calculated with the following formula: toe swelling = post-inflammatory volume – pre-inflammatory volume.²⁷ The arthritis index (AI) was calculated. Specifically, systemic lesions were evaluated with a 5-grade scoring method: 0 scores, no swelling of the joints; 1 score, joint redness and swelling in the little toe; 2 scores, redness and swelling of the toes joints and the footpad; 3 scores, redness and swelling of the ankle joints and the whole foot claw; 4 scores, redness and swelling of the ankle joints and the whole foot claw and even joint deformity. The AI of each rat was obtained based on the cumulative score of the degree of lesions in the remaining 3 limbs that were not injected with FCA and calculated by accumulating the score of each joint, with a maximum score of 12.²⁸

Collection of Myocardial and Synovial Tissues and Blood Samples

After the assessment of arthritis severity, rats were anesthetized through the intraperitoneal injection of 3% sodium pentobarbital (30 mg/kg) and then euthanized. The synovial and myocardial tissues of rats were separated, of which some were stored at -80°C for RT-qPCR and Western blotting, and the rest were fixed in 4% paraformaldehyde and preserved at room temperature for pathological detection. Blood samples were obtained through abdominal aortic puncture with

vacuum blood collection tubes and centrifuged at 3000 r/min for 5 min, followed by the collection of the supernatant. Then, the supernatant was stored at -80°C for cytokine assays.

HE Staining

The synovial and myocardial tissues were fixed in 4% paraformaldehyde, followed by dehydration, clearing, and wax embedding. Next, the tissues were cut into 6 μm sections for HE staining. Finally, the pathological and morphological changes of rat synovium and myocardium were observed under the microscope.

Transmission Electron Microscopy (TEM)

The sections of myocardial tissues were fixed in Eppendorf tubes containing fixative for electron microscopy, washed with phosphate-buffered saline three times (15 min each time), followed by fixation with 1% osmic acid for 2 h at room temperature in dark and three rinses. After dehydration, permeation, embedding, and ultrathin sectioning, TEM was conducted to observe the ultrastructural changes of tissues, and photographs were taken.

ELISA

The serum levels of IL-1 β , IL-6, IL-18, and TNF- α were measured as instructed in the manuals of ELISA kits.

LDH Assay

LDH release from rat myocardial tissues was tested as per the protocols of the LDH kit.

RT-qPCR

The total RNA of rat myocardial tissues was extracted according to the manuals of the TRIzol Kit. cDNA was obtained through reverse transcription of RNA with a reverse transcription kit and amplified with a SYBR Green kit. Reaction conditions were set at the different stages and included denaturation at 95°C for 3 min and 40 cycles of PCRs at 95°C for 15s and at 60°C for 30s. Glyceraldehyde-3-phosphate dehydrogenase and U6 were used as internal references for miR-21 and other genes, respectively, and the relative gene expression was calculated with the $2^{-\Delta\Delta\text{Ct}}$ method. The used primers are listed in Table 1.

Western Blotting

Rat myocardial tissues were lysed and homogenized, and the supernatant was attained, followed by the measurement of the protein concentration with a protein concentration assay kit. Protein samples were added with the appropriate amount of diluents and sampling buffer, separated through 10% sodium dodecyl sulfate–polyacrylamide gel electrophoresis, and transferred into polyvinylidene fluoride membranes. After being sealed, the membranes were subjected to overnight incubation with primary antibodies anti-TLR4 (1:1000), anti-NF- κB p65 (1:1000), anti-GSDMD (1:500), anti-Caspase-1 (1:500), and anti-NLRP3 (1:1000) at 4°C overnight, Tris-Buffered Saline with Tween 20 (TBST) washing, 2 h incubation with secondary antibodies, and TBST washing. After that, the membranes were added with Enhanced Chemiluminescence Plus solutions, followed by rapid development and exposure. The grayscale of images was analyzed with ImageJ software. Anti- β -actin (1:5000) was used as reference protein for normalization. The relative expression of target proteins was calculated by the ratio of the grayscale value of target proteins to that of the internal reference β -actin.

Statistical Analysis

Data were analyzed with GraphPad Prism 9.5.1 (GraphPad Institute, San Diego, CA, USA) software and summarized as mean \pm standard deviation. Data with normality and homogeneity of variance were compared between two groups with the *t*-test and among multiple groups with one-way analysis of variance. Differences were statistically significant at $P < 0.05$.

Table 1 Primer Used for RT-qPCR

Targets	Sequences
LncRNA GAS5	Forward: 5'-AAGCTCCACACAAGGTCCTT-3' Reverse: 5'-GCATCCATCCAGTCACCTCT-3'
NLRP3	Forward: 5'-GAAACTCTGGTTGGTCAGC-3' Reverse: 5'-AGAGAATGGGTTGGAGCTCAG-3'
GSDMD	Forward: 5'-CGACTCTGGAGAACTGGTG-3' Reverse: 5'-TGGGTTTCACTCAACCCAG-3'
Caspase-1	Forward: 5'-AAGATGATGGCATTAGAAGGC-3' Reverse: 5'-TCCAGGACACATTATCTGGTG-3'
TLR4	Forward: 5'-CCTGCATAGAGGTACTTCCT-3' Reverse: 5'-AATAAGGGGATGTCATGAGGGA-3'
NF-κB p65	Forward: 5'-TGTGAAGAAGCGAGACCTG-3' Reverse: 5'-TCCTCTATGGAACTTGAAAGG-3'
GAPDH	Forward: 5'-AGGTCGGGTGTGAACGGATTG-3' Reverse: 5'-GGGGTCGTTGATGGCAACA-3'
miR-21	Forward: 5'-GCGCGTAGCTTATCAGACTGA-3' Reverse: 5'-AGTGCAGGGTCCGAGGTATT-3'
miR-21 (reverse transcription) U6	5'-GTCGTATCCAGTGCAGGGTCCGAGGTATTTCGCACTGGATACGACTCAACA-3' Forward: 5'-CTCGCTTCGGCAGCAC-3' Reverse: 5'-AACGCTTCACGAATTTGCGT-3'

Results

XFC Reduces Toe Swelling and AI Scores in AA Rats

Compared with those in the NC group, toe swelling and AI scores in other groups peaked on the 1st day after inflammation induction, decreased to the lowest level on the 8th day, and gradually increased from the 11th day. Drug interventions were started on day 19 after inflammation induction. In XFC treatment groups, toe swelling was reduced from day 29, and AI scores declined from day 22, highlighting that XFC ameliorated toe swelling and joint inflammation in AA rats (Figure 1).

XFC Attenuates Synovial and Myocardial Tissue Damage in AA Rats

HE staining was performed to assess synovial and myocardial tissue damage in AA rats. The results revealed that in the NC group, rat synovial tissues showed normal cell growth, without synovial thickening and fibrosis and inflammatory cell infiltration, and rat myocardial tissues were structurally intact, with neatly aligned fibers, uniform and clear cell nucleus staining, and no edema and inflammatory cell infiltration. Compared with those in the NC group, rat synovial tissues in the MC group had unclear layers, with thickening and fibrosis, visible angiogenesis, and massive inflammatory cell infiltration, and rat myocardial tissues in the MC group were damaged, accompanied by broken and lysed myocardial fibers, widened gaps, inhomogeneous cell nucleus staining, cellular edema, and massive inflammatory cells infiltration. The pathological state of rat synovial and myocardial tissues in the AA group was improved by treatment with XFC or MTX. Compared with the XFC group, the XFC + GAS5 and XFC + NSA groups had a significantly improved pathological state of rat synovial and myocardial tissues (Figure 2).

XFC Improves the Ultrastructure of Myocardial in AA Rats

The ultrastructure of rat myocardial was observed with TEM. In the NC group, the morphology and structure of cardiomyocytes were normal and myofibrils were arranged regularly and clearly, with complete mitochondrial morphology, clear structure of mitochondrial cristae, and no obvious pyroptotic vesicles. Compared with the NC group, the MC group exhibited broken cell membranes and pore formation of rat cardiomyocytes, poorly arranged myofibrils, broken and sparse mitochondrial cristae, and a large number of pyroptotic vesicles. Treatment with MTX or XFC improved the

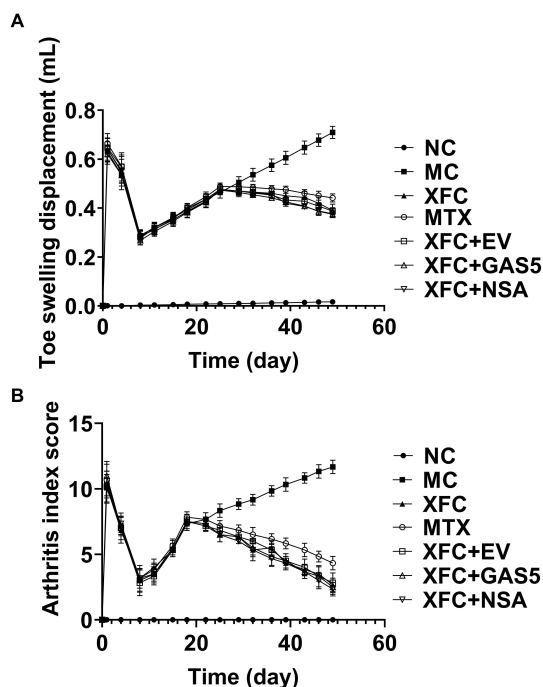


Figure 1 Effect of XFC on toe swelling and arthritis index in AA rats.

Notes: (A) Toe swelling degree of rats in each group. (B) Arthritis index of rats in each group. NC, the normal control group; MC, the model control group; XFC, the Xinfeng Capsule group; MTX, the methotrexate tablet group; XFC + EV, the Xinfeng Capsule + empty AAV group; XFC + GAS5, the Xinfeng Capsule + AAV harboring GAS5 overexpression group; XFC + NSA, the Xinfeng Capsule + NSA (a pyroptosis inhibitor) group. n=number of rats (6 rats/group).

ultrastructure of myocardial in AA rats, which was further markedly improved in the XFC + GAS5 and XFC + NSA groups (Figure 3).

XFC Diminishes Serum Pro-Inflammatory Cytokine Levels in AA Rats

The serum levels of pro-inflammatory cytokines in rats were examined with ELISA. The serum levels of IL-1 β , IL-18, IL-6, and TNF- α were substantially higher in the MC group than in the NC group ($P < 0.01$) and greatly lower in the XFC and MTX groups than in the MC group ($P < 0.01$, $P < 0.05$). Compared with the XFC group, the XFC + GAS5 and XFC + NSA groups showed a significant decrease in the serum levels of IL-1 β , IL-18, IL-6, and TNF- α ($P < 0.01$, $P < 0.05$) (Figure 4). Overall, XFC could effectively decline the serum levels of pro-inflammatory cytokines in AA rats, which was further promoted by GAS5 overexpression and NSA.

XFC Depresses LDH Release in AA Rats

LDH release was detected to evaluate pyroptosis. LDH release in the MC group was significantly increased compared with that in the NC group ($P < 0.01$), whereas LDH release in the XFC and MTX groups was substantially lowered as compared to that in the MC group ($P < 0.01$, $P < 0.05$). In contrast to the XFC group, LDH release was prominently diminished in the XFC + GAS5 and XFC + NSA groups ($P < 0.01$) (Figure 5). In summary, XFC could effectively inhibit LDH release in AA rats, and this effect was fueled by GAS5 overexpression or NSA.

XFC Modulates the GAS5/miR-21/TLR4 Axis and Pyroptosis-Related Indicators in Myocardial Tissues of AA Rats

The expression of the GAS5/miR-21/TLR4 axis and pyroptosis-related indicators were tested in rat myocardial tissues. The expression of miR-21, TLR4, NF- κ B p65, NLRP3, Caspase-1, and GSDMD was greatly enhanced and GAS5 expression was markedly reduced in the MC group versus the NC group ($P < 0.01$), whilst opposite trends were observed in the XFC and MTX groups as compared to the MC group ($P < 0.01$, $P < 0.05$). Relative to the XFC group, the XFC +

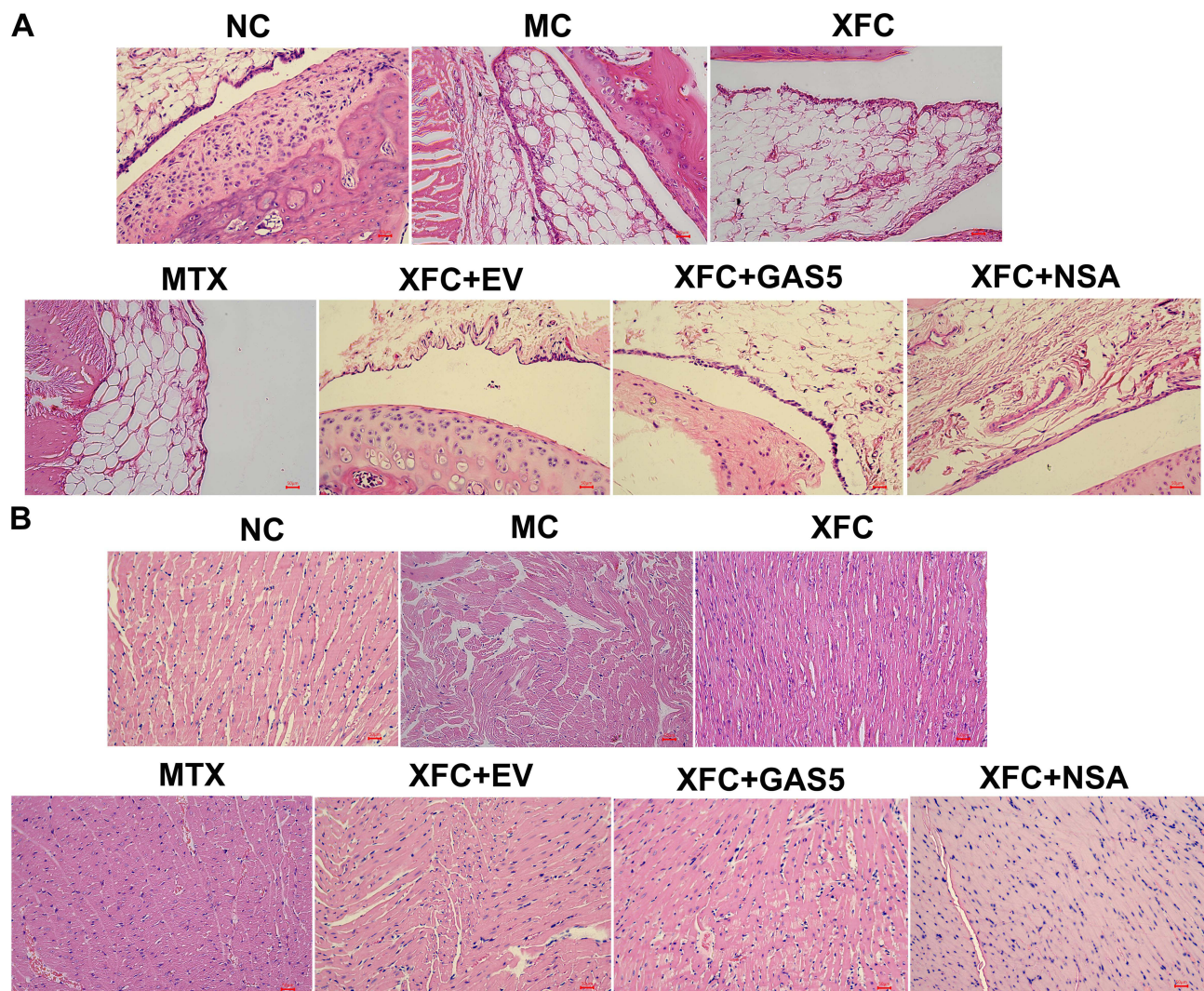


Figure 2 Effects of XFC on the histopathology of synovium and myocardium in AA rats (HE, $\times 200$).

Notes: (A) Synovial histopathology of rats. (B) Myocardial histopathology of rats. NC, the normal control group; MC, the model control group; XFC, the Xinfeng Capsule group; MTX, the methotrexate tablet group; XFC + EV, the Xinfeng Capsule + empty AAV group; XFC + GAS5, the Xinfeng Capsule + AAV harboring GAS5 overexpression group; XFC + NSA, the Xinfeng Capsule + NSA (a pyroptosis inhibitor) group.

GAS5 and XFC + NSA groups had significantly higher GAS5 expression and substantially poorer expression of miR-21, TLR4, NF- κ B p65, NLRP3, Caspase-1, and GSDMD ($P < 0.01$) (Figure 6A–C). In conclusion, XFC could up-regulate GAS5 expression and down-regulate miR-21, TLR4, NF- κ B p65, and pyroptosis-related indicators in myocardial tissues of AA rats, which was further promoted by GAS5 overexpression or NSA.

Discussion

As a systemic autoimmune disease, RA mainly manifests as chronic inflammation of joint synovial tissues.²⁹ Molecular mechanisms underlying RA remain unexclusive although the development of RA has been reported to share an association with risk factors including genetic, environmental, and immunologic factors.³⁰ RA patients are prevalently complicated by CVD, particularly cardiac lesions.³¹ Therefore, it is of tremendous importance to search for new therapeutic approaches for preventing and controlling the progression of RA toward serious cardiovascular events. The present study explored the mechanism of XFC in treating RA myocardial injury through the establishment of an AA rat model to provide potential targets in improving the management of myocardial injury in RA. It was observed that toe swelling and AI scores were substantially elevated in rats after AA modeling. The pathological observation of synovial

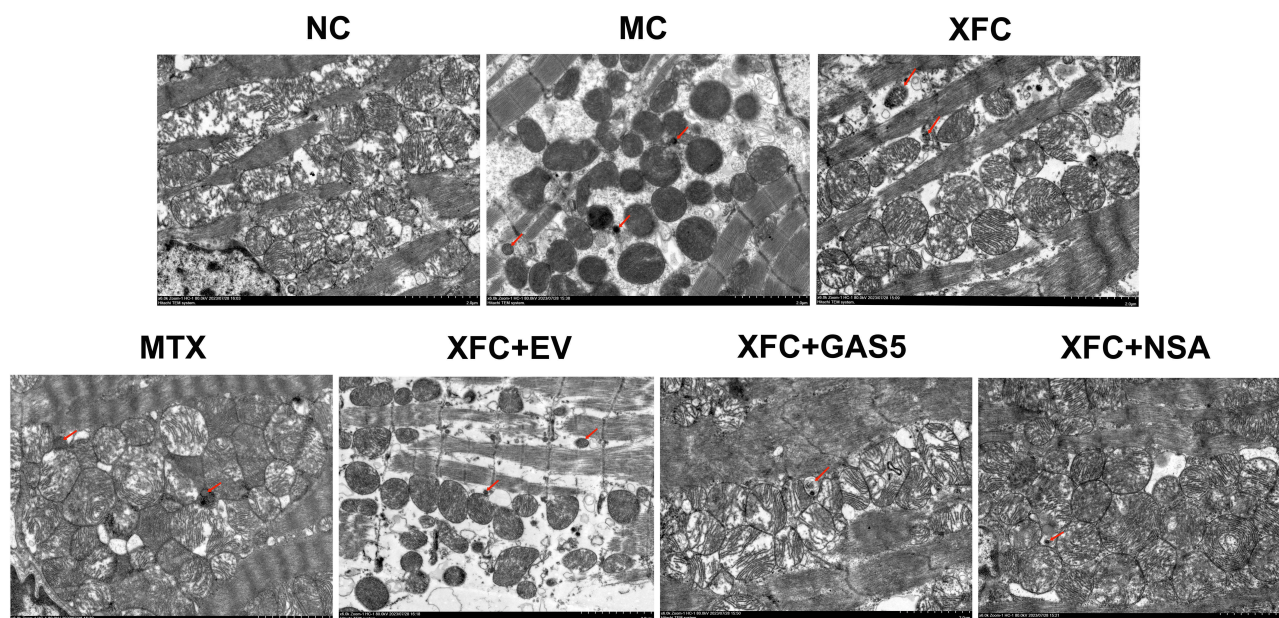


Figure 3 Effects of XFC on the ultrastructure of myocardial in AA rats (TEM, $\times 6000$).

Notes: The ultrastructure of the myocardium in different groups of rats is shown in the figure. The red arrow refers to the pyroptotic vesicles. NC, the normal control group; MC, the model control group; XFC, the Xinfeng Capsule group; MTX, the methotrexate tablet group; XFC + EV, the Xinfeng Capsule + empty AAV group; XFC + GAS5, the Xinfeng Capsule + AAV harboring GAS5 overexpression group; XFC + NSA, the Xinfeng Capsule + NSA (a pyroptosis inhibitor) group.

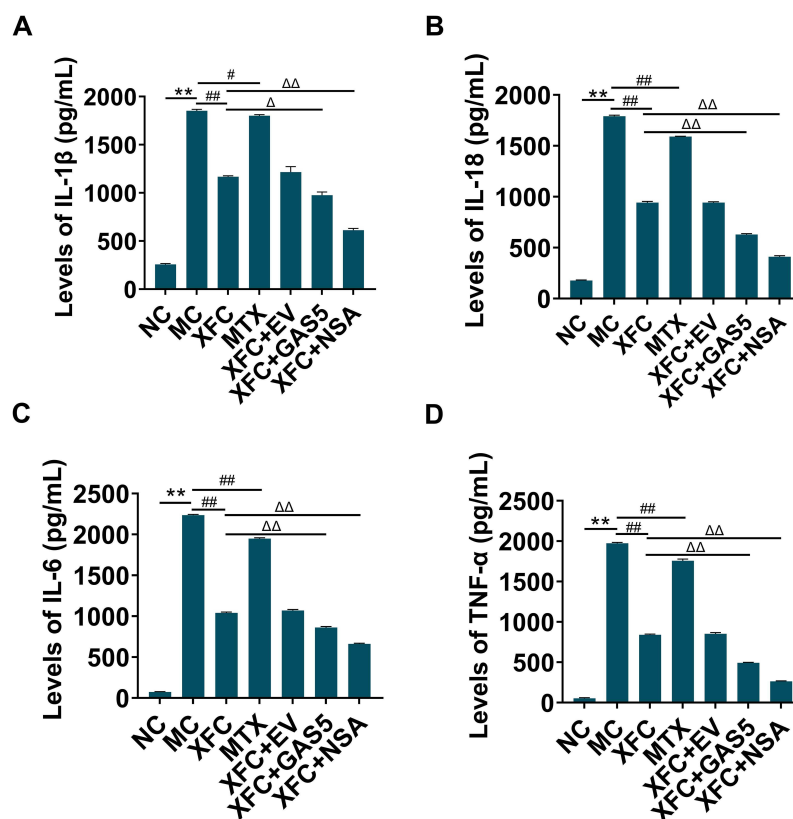


Figure 4 Effect of XFC on serum cytokines in AA rats.

Notes: (A) IL-1 β levels in different groups. (B) IL-18 levels in different groups. (C) IL-6 levels in different groups. (D) TNF- α levels in different groups. NC, the normal control group; MC, the model control group; XFC, the Xinfeng Capsule group; MTX, the methotrexate tablet group; XFC + EV, the Xinfeng Capsule + empty AAV group; XFC + GAS5, the Xinfeng Capsule + AAV harboring GAS5 overexpression group; XFC + NSA, the Xinfeng Capsule + NSA (a pyroptosis inhibitor) group. Values are mean \pm standard deviation, n=number of rats (6 rats/group). ** $P < 0.01$, compared with the NC group; ### $P < 0.01$, # $P < 0.05$, compared with the MC group; $\Delta\Delta P < 0.01$, $\Delta P < 0.05$, compared with the XFC group.

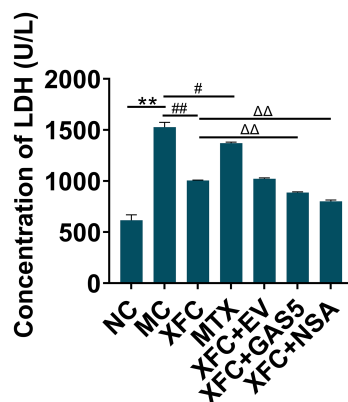


Figure 5 Effect of XFC on LDH release from myocardial tissues in AA rats.

Notes: The graph displays the statistical analysis results of LDH release from rat myocardial tissues in different groups. NC, the normal control group; MC, the model control group; XFC, the Xinfeng Capsule group; MTX, the methotrexate tablet group; XFC + EV, the Xinfeng Capsule + empty AAV group; XFC + GAS5, the Xinfeng Capsule + AAV harboring GAS5 overexpression group; XFC + NSA, the Xinfeng Capsule + NSA (a pyroptosis inhibitor) group. Values are mean \pm standard deviation, n=number of rats (6 rats/group). ** $p < 0.01$, compared with the NC group; ## $p < 0.01$, # $p < 0.05$, compared with the MC group; $\Delta\Delta p < 0.01$, compared with the XFC group.

tissues showed that the synovium of AA rats showed active hyperplasia, obvious inflammatory cell infiltration, and pannus formation. Further pathological observation of myocardial tissues unveiled that myocardial fibers were broken and lysed and the membrane of cardiomyocytes was broken with pore formation, accompanied by obviously broken and sparse mitochondrial cristae and massive inflammatory cell infiltration and pyroptotic vesicles. This finding implies that AA rats presented with both joint inflammation and myocardial tissue inflammation and damage. In RA, myocardial injury may be secondary to inflammation. XFC treatment significantly decreased toe swelling, AI scores, and pathological damage and inflammation of synovial and myocardial tissues in AA rats, indicating the therapeutic effect of XFC on joint inflammation and myocardial injury in AA rats.

As a newly discovered form of inflammatory cell death, pyroptosis is primarily associated with pathways including Caspase-1, Caspase-4/5/11-dependent pathway, and Caspase-3/8-mediated novel pathway.⁷ Wu et al⁸ found that Pentraxin 3, a new diagnostic marker for RA, activated NLRP3 inflammasomes and Caspase-1 and induced cleavage of GSDMD and secretion of cytokines such as IL-1 β , IL-18, IL-6, and TNF- α in a C1q-dependent manner to promote monocyte pyroptosis in RA patients, accompanied by an increase in LDH release. Li et al³² observed that TLR4, NLRP3, Caspase-1, GSDMD, and IL-1 β expression was increased in knee joints and the LDH activity was augmented in the serum of rats with a modified adjuvant-induced arthritis model. In addition, He et al³³ also measured high levels of Caspase-1, GSDMD, NLRP3, IL-1 β , and IL-18 and high serum activity of LDH in mice with ischemia-reperfusion injury. Importantly, another study elucidated that targeted inhibition of NLRP3 inflammasome-mediated pyroptosis could attenuate myocardial injury.³⁴ Consistently, the current study revealed a significant increase in the levels of pro-inflammatory cytokines including IL-1 β , IL-18, IL-6, and TNF- α in the serum and a marked elevation in the levels of pyroptosis-related indicators Caspase-1, GSDMD, and NLRP3 in myocardial tissues of AA rats, illustrating the presence of immune-inflammatory responses and cardiomyocyte pyroptosis in AA rats and that RA-related myocardial injury may be related to the release of pro-inflammatory cytokines and the initiation of the pyroptosis pathway. In our study, XFC treatment greatly decreased the expression of IL-1 β , IL-18, IL-6, TNF- α , NLRP3, Caspase-1, and GSDMD and the release of LDH, highlighting that XFC may attenuate myocardial injury in AA rats by repressing pro-inflammatory cytokines and pyroptosis.

GAS5 was originally discovered through screening of potential tumor suppressors.³⁵ Reportedly, GAS5 is associated with several autoimmune diseases, including RA.¹⁹ Accumulating studies have unraveled that GAS5 is poorly expressed in RA patients, mice, and fibroblast-like synoviocytes (FLSs).^{36–38} For example, Wu et al³⁶ detected low expression of GAS5 in peripheral blood mononuclear cells of RA patients and confirmed a negative correlation between GAS5 and C-reactive protein. Chen et al³⁷ noted that GAS5 reduced the levels of pro-inflammatory cytokines and oxidative stress-related parameters, thus mitigating synovial inflammation and bone destruction in RA mice. The research by Li et al³⁸ elaborated that GAS5 knockdown accelerated RA-FLS proliferation by activating the phosphatidylinositol 3-kinase/

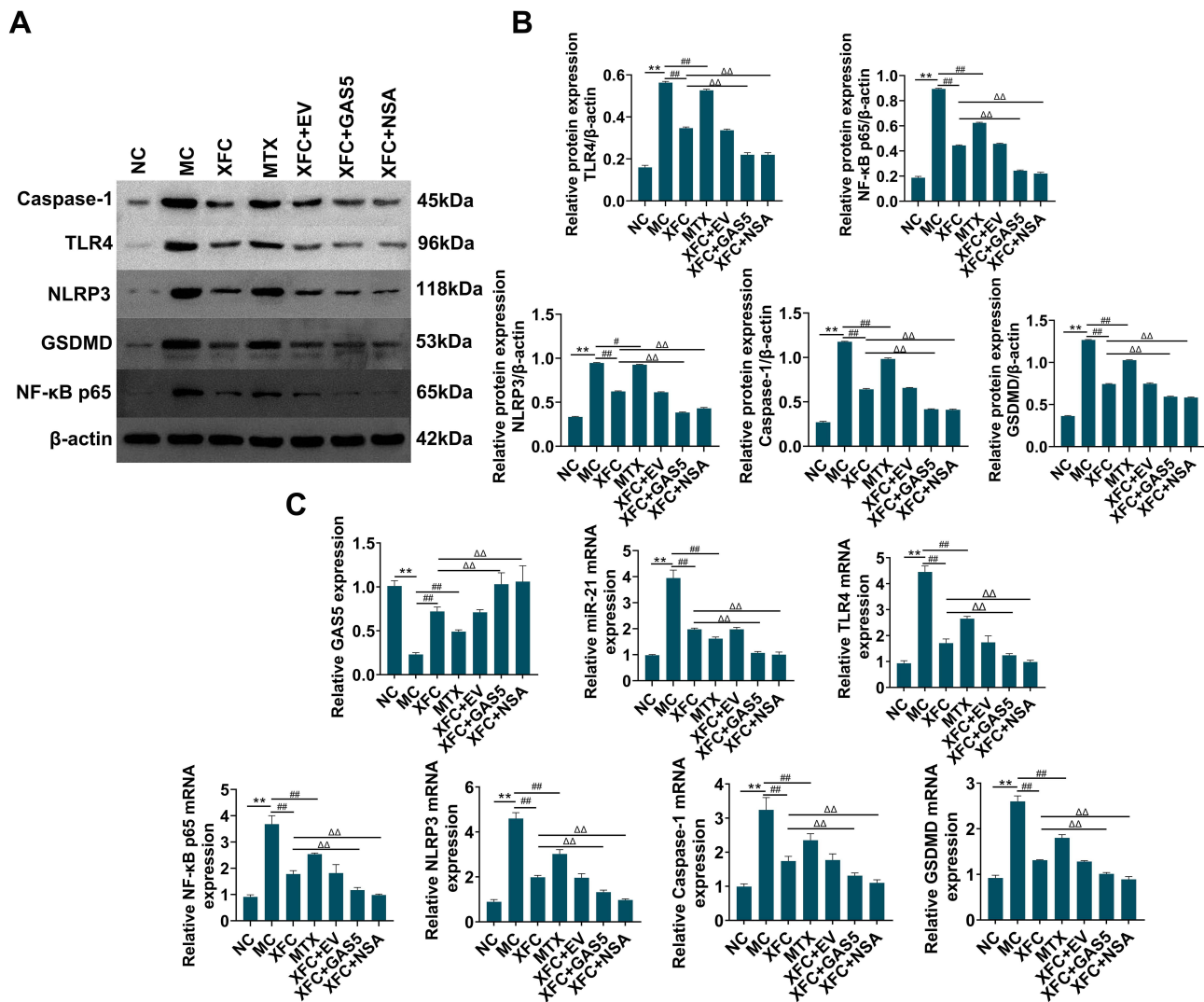


Figure 6 Effects of XFC on the expression of the GASS5/miR-21/TLR4 axis and pyroptosis-related indicators in myocardial tissues of AA rats.

Notes: (A) Protein levels of TLR4, NF-κB p65, NLRP3, Caspase-1, and GSDMD in rat myocardial tissues. (B) Semi-quantitative analysis of protein levels. (C) Expression of GASS5 and mRNA expression of miR-21, TLR4, NF-κB p65, NLRP3, Caspase-1, and GSDMD in rat myocardial tissues. NC, the normal control group; MC, the model control group; XFC, the Xinfeng Capsule group; MTX, the methotrexate tablet group; XFC + EV, the Xinfeng Capsule + empty AAV group; XFC + GAS5, the Xinfeng Capsule + AAV harboring GAS5 overexpression group; XFC + NSA, the Xinfeng Capsule + NSA (a pyroptosis inhibitor) group. Values are mean ± standard deviation, n=number of rats (6 rats/group). ** $P < 0.01$, compared with the NC group; ### $P < 0.01$, # $P < 0.05$, compared with the MC group; $\Delta\Delta P < 0.01$, compared with the XFC group.

protein kinase B pathway. Furthermore, GAS5-mediated ceRNA regulatory pathways have been demonstrated to influence cardiomyocyte pyroptosis.¹⁸ GAS5 and miR-21 have negative regulatory mechanisms in vitro and in vivo. For instance, GAS5 acts as a sponge to directly bind to miR-21 via putative miRNA response elements.^{39,40} miR-21 down-regulation prevents not only Caspase-1 activation but also GSDMD cleavage-induced pyroptosis.²² In addition, TLR4, as a potential target gene of miR-21,²¹ can block the NF-κB/NLRP3 pathway to modulate pyroptosis and diminish RA activity.⁴¹ Combined with our previous findings,^{25,42} we hypothesized that RA-related myocardial injury might be associated with the abnormal activation of the GAS5/miR-21/TLR4 axis, the initiation of the pyroptosis pathway, and the secretion of pro-inflammatory cytokines. Our results exhibited substantial decreases in GAS5 expression and significant elevations in the expression of miR-21 and its downstream target gene TLR4 and NF-κB p65 in myocardial tissues of AA rats, suggesting that GAS5, miR-21, and TLR4 were differentially expressed in the myocardial tissues of AA rats and that GAS5 expression was negatively correlated with miR-21 and TLR4 expression. XFC intervention prominently enhanced GAS5 expression and lowered miR-21, TLR4 and NF-κB p65 expression. In the presence of XFC intervention, miR-21, TLR4 and NF-κB p65 expression was significantly decreased in the myocardial tissues of AA rats by GAS5

overexpression or NSA (the pyroptosis inhibitor), accompanied by lowered serum levels of IL-1 β , IL-18, IL-6, and TNF- α and diminished LDH release and NLRP3, Caspase-1, and GSDMD expression in myocardial tissues, pathological damage of synovial and myocardial tissues significant improvement, illustrating that GAS5 may down-regulate TLR4 by binding to and negatively regulating miR-21, thus suppressing myocardial pyroptosis in AA rats. Overall, XFC may lower the expression of pro-inflammatory cytokines and pyroptosis-related indicators via the GAS5/miR-21/TLR4 axis, therefore ameliorating myocardial injury in AA rats. However, it is uncertain about the involvement of other genes or modified proteins in this process, which is the direction of our future research.

Conclusion

XFC reduced toe swelling, AI scores, the serum levels of pro-inflammatory cytokine, LDH release, and the expression of miR-21, TLR4, NF- κ B p65, and pyroptosis-related indicators while enhancing GAS5 expression, hence repressing inflammation in synovial and myocardial tissues, and attenuating cardiomyocyte pyroptosis in AA rats. Conclusively, the TCM compound preparation XFC ameliorated myocardial injury in AA rats by mediating the GAS5/miR-21/TLR4 axis, inhibiting pyroptosis, and down-regulating pro-inflammatory cytokines.

Ethical Approval

All animal experiments were accordance with The Guide for Care and Use of Laboratory Animals released by National Institutes of Health and approved by the Animal Ethics Committee of the Anhui University of Chinese Medicine (Approval No. AHUCM-rats-2023033).

Acknowledgments

We would like to acknowledge the reviewers for their helpful comments on this paper.

Funding

This study was partially supported by the General project of the National Natural Science Foundation of China (82074090); High level Key Discipline Construction Project of TCM of the State Administration of TCM (Guozhong Pharmaceutical Education Letter [2023] No. 85); National TCM Inheritance and Innovation Center Project (Development and Reform Office Social [2022] No. 366); Anhui Provincial Natural Science Foundation Project (2208085MH267); Anhui Province Higher Education Science Research Project (2023AH050732); The seventh batch of national academic experience inheritance projects for elderly TCM experts (Guozhong Pharmaceutical Education Letter [2022] No. 76); Anhui Province Graduate Education Quality Engineering Project (2022 cxcysj133).

Disclosure

The authors report no conflicts of interest in this work.

References

1. Kondo N, Kanai T, Okada M. Rheumatoid arthritis and reactive oxygen species: a review. *Curr Issues Mol Biol.* 2023;45(4):3000–3015. doi:10.3390/cimb45040197
2. Marcucci E, Bartoloni E, Alunno A, et al. Extra-articular rheumatoid arthritis. *Reumatismo.* 2018;70(4):212–224. doi:10.4081/reumatismo.2018.1106
3. Guo Y, Chung W, Shan Z, Zhu Z, Costenbader KH, Liang L. Genome-wide assessment of shared genetic architecture between rheumatoid arthritis and cardiovascular diseases. *J Am Heart Assoc.* 2023;e030211. doi:10.1161/jaha.123.030211
4. Løgstrup BB, Ellingsen T, Pedersen AB, et al. Cardiovascular risk and mortality in rheumatoid arthritis compared with diabetes mellitus and the general population. *Rheumatology.* 2021;60(3):1400–1409. doi:10.1093/rheumatology/keaa374
5. Stainer A, Tonutti A, De Santis M, et al. Unmet needs and perspectives in rheumatoid arthritis-associated interstitial lung disease: a critical review. *Front Med.* 2023;10:1129939. doi:10.3389/fmed.2023.1129939
6. Shi J, Gao W, Shao F. Pyroptosis: gasdermin-mediated programmed necrotic cell death. *Trends Biochem Sci.* 2017;42(4):245–254. doi:10.1016/j.tibs.2016.10.004
7. You R, He X, Zeng Z, Zhan Y, Xiao Y, Xiao R. Pyroptosis and Its Role in Autoimmune Disease: a Potential Therapeutic Target. *Front Immunol.* 2022;13:841732. doi:10.3389/fimmu.2022.841732
8. Wu XY, Li KT, Yang HX, et al. Complement C1q synergizes with PTX3 in promoting NLRP3 inflammasome over-activation and pyroptosis in rheumatoid arthritis. *J Autoimmun.* 2020;106:102336. doi:10.1016/j.jaut.2019.102336

9. Tian K, Yang Y, Zhou K, et al. The role of ROS-induced pyroptosis in CVD. *Front Cardiovasc Med.* 2023;10:1116509. doi:10.3389/fcvm.2023.1116509
10. Zhaolin Z, Guohua L, Shiyuan W, Zuo W. Role of pyroptosis in cardiovascular disease. *Cell Prolif.* 2019;52(2):e12563. doi:10.1111/cpr.12563
11. Robinson EK, Covarrubias S, Carpenter S. The how and why of lncRNA function: an innate immune perspective. *Biochim Biophys Acta Gene Regul Mech.* 2020;1863(4):194419. doi:10.1016/j.bbgrm.2019.194419
12. Bhan A, Mandal SS. Long noncoding RNAs: emerging stars in gene regulation, epigenetics and human disease. *ChemMedChem.* 2014;9(9):1932–1956. doi:10.1002/cmdc.201300534
13. Hur K, Kim SH, Kim JM. Potential implications of long noncoding RNAs in autoimmune diseases. *Immune Netw.* 2019;19(1):e4. doi:10.4110/in.2019.19.e4
14. Mao Q, Liang XL, Zhang CL, Pang YH, Lu YX. LncRNA KLF3-AS1 in human mesenchymal stem cell-derived exosomes ameliorates pyroptosis of cardiomyocytes and myocardial infarction through miR-138-5p/Sirt1 axis. *Stem Cell Res Ther.* 2019;10(1):393. doi:10.1186/s13287-019-1522-4
15. Ma S, Zhao H, Wang F, et al. Integrative analysis to screen novel pyroptosis-related lncRNAs for predicting clinical outcome of glioma and validation in tumor tissue. *Aging.* 2023;15(5):1628–1651. doi:10.18632/aging.204580
16. Han JJ, Wang XQ, Zhang XA. Functional interactions between lncRNAs/circRNAs and miRNAs: insights into rheumatoid arthritis. *Front Immunol.* 2022;13:810317. doi:10.3389/fimmu.2022.810317
17. Wang M, An G, Wang B, et al. Integrated analysis of the lncRNA-miRNA-mRNA network based on competing endogenous RNA in atrial fibrillation. *Front Cardiovasc Med.* 2023;10:1099124. doi:10.3389/fcvm.2023.1099124
18. Zheng Y, Zhang Y, Zhang X, et al. Novel lncRNA-miRNA-mRNA competing endogenous RNA triple networks associated programmed cell death in heart failure. *Front Cardiovasc Med.* 2021;8:747449. doi:10.3389/fcvm.2021.747449
19. Wu H, Chen S, Li A, et al. LncRNA expression profiles in systemic lupus erythematosus and rheumatoid arthritis: emerging biomarkers and therapeutic targets. *Front Immunol.* 2021;12:792884. doi:10.3389/fimmu.2021.792884
20. Shen Y, Xu J, Zhi S, et al. MIP from legionella pneumophila Influences the phagocytosis and chemotaxis of RAW264.7 macrophages by regulating the lncRNA GAS5/miR-21/SOCS6 axis. *Front Cell Infect Microbiol.* 2022;12:810865. doi:10.3389/fcimb.2022.810865
21. Liu XJ, Lv JL, Zou X, et al. MiR-21 alleviates renal tubular epithelial cells injury induced by ischemia by targeting TLR4. *Heliyon.* 2023;9(5):e15818. doi:10.1016/j.heliyon.2023.e15818
22. Xue Z, Xi Q, Liu H, et al. miR-21 promotes NLRP3 inflammasome activation to mediate pyroptosis and endotoxic shock. *Cell Death Dis.* 2019;10(6):461. doi:10.1038/s41419-019-1713-z
23. Yin Y, Wu X, Peng B, et al. Curcumin improves necrotising microscopic colitis and cell pyroptosis by activating SIRT1/NRF2 and inhibiting the TLR4 signalling pathway in newborn rats. *Innate Immun.* 2020;26(7):609–617. doi:10.1177/1753425920933656
24. Choulaki C, Papadaki G, Repa A, et al. Enhanced activity of NLRP3 inflammasome in peripheral blood cells of patients with active rheumatoid arthritis. *Arthritis Res Ther.* 2015;17(1):257. doi:10.1186/s13075-015-0775-2
25. Cao YX, Huang D, Liu J, et al. A Novel Chinese Medicine, Xinfeng Capsule, Modulates Proinflammatory Cytokines via Regulating the Toll-Like Receptor 4 (TLR4)/Mitogen-Activated Protein Kinase (MAPK)/Nuclear Kappa B (NF-κB) signaling pathway in an adjuvant arthritis rat model. *Med Sci Monit.* 2019;25:6767–6774. doi:10.12659/msm.916317
26. Liu J, Cao Y, Huang C, et al. Use of xinfeng capsule to treat articular pathologic changes in patients with rheumatoid arthritis. *J Tradit Chin Med.* 2014;34(5):532–538. doi:10.1016/s0254-6272(15)30058-3
27. Chen J, Wang W, Jiang M, Yang M, Wei W. Combination therapy of ginsenoside compound K and methotrexate was efficient in elimination of anaemia and reduction of disease activity in adjuvant-induced arthritis rats. *Pharm Biol.* 2020;58(1):1131–1139. doi:10.1080/13880209.2020.1844761
28. Li F, Dai M, Wu H, et al. Immunosuppressive effect of geniposide on mitogen-activated protein kinase signalling pathway and their cross-talk in fibroblast-like synoviocytes of adjuvant arthritis rats. *Molecules.* 2018;23(1). doi:10.3390/molecules23010091
29. Sun J, Zhai W, Wang Z, An W. Methotrexate plus electroacupuncture reduces autophagy in ankle synovial tissue in rats with rheumatoid arthritis. *Am J Transl Res.* 2023;15(4):2747–2756.
30. Karami J, Aslani S, Jamshidi A, Garshasbi M, Mahmoudi M. Genetic implications in the pathogenesis of rheumatoid arthritis; an updated review. *Gene.* 2019;702:8–16. doi:10.1016/j.gene.2019.03.033
31. Jin S, Zhao J, Li M, Zeng X. New insights into the pathogenesis and management of rheumatoid arthritis. *Chronic Dis Transl Med.* 2022;8(4):256–263. doi:10.1002/cdt3.43
32. Li W, Mao X, Wang X, et al. Disease-modifying anti-rheumatic drug prescription baihu-guizhi decoction attenuates rheumatoid arthritis via suppressing toll-like receptor 4-mediated NLRP3 inflammasome activation. *Front Pharmacol.* 2021;12:743086. doi:10.3389/fphar.2021.743086
33. He W, Duan L, Zhang L. LOXL1-AS1 aggravates myocardial ischemia/reperfusion injury through the miR-761/Pten axis. *Korean Circ J.* 2023;53(6):387–403. doi:10.4070/kcj.2022.0301
34. Chen X, Tian C, Zhang Z, et al. Astragaloside IV inhibits NLRP3 inflammasome-mediated pyroptosis via activation of Nrf-2/HO-1 signaling pathway and protects against doxorubicin-induced cardiac dysfunction. *Front Biosci.* 2023;28(3):45. doi:10.31083/j.fbl2803045
35. Zhou L, Jiang H, Lin L, Li Y, Li J. lncRNA GAS5 suppression of the malignant phenotype of ovarian cancer via the miR-23a-WT1 axis. *Ann Transl Med.* 2023;11(2):119. doi:10.21037/atm-22-6394
36. Wu J, Zhang TP, Zhao YL, et al. Decreased H19, GAS5, and linc0597 expression and association analysis of related gene polymorphisms in rheumatoid arthritis. *Biomolecules.* 2019;10(1):55. doi:10.3390/biom10010055
37. Chen H, He C, Liu Y, et al. LncRNA-GAS5 inhibits expression of miR 103 and ameliorates the articular cartilage in adjuvant-induced arthritis in obese mice. *Dose Response.* 2020;18(4):1559325820942718. doi:10.1177/1559325820942718
38. Li G, Liu Y, Meng F, et al. Tanshinone IIA promotes the apoptosis of fibroblast-like synoviocytes in rheumatoid arthritis by up-regulating lncRNA GAS5. *Biosci Rep.* 2018;38(5):BSR20180626. doi:10.1042/bsr20180626
39. Geng X, Song N, Zhao S, et al. LncRNA GAS5 promotes apoptosis as a competing endogenous RNA for miR-21 via thrombospondin 1 in ischemic AKI. *Cell Death Discov.* 2020;6:19. doi:10.1038/s41420-020-0253-8
40. Cong C, Tian J, Gao T, et al. lncRNA GAS5 is upregulated in osteoporosis and downregulates miR-21 to promote apoptosis of osteoclasts. *Clin Interv Aging.* 2020;15:1163–1169. doi:10.2147/cia.S235197

41. Li W, Wang K, Liu Y, et al. A novel drug combination of mangiferin and cinnamic acid alleviates rheumatoid arthritis by inhibiting TLR4/NFκB/NLRP3 activation-induced pyroptosis. *Front Immunol.* 2022;13:912933. doi:10.3389/fimmu.2022.912933
42. Cao Y, Guo Y, Wang Y, et al. Drug-containing serum of Xinfeng capsules protect against H9C2 from death by enhancing miRNA-21 and inhibiting toll-like receptor 4/phosphorylated p-38 (p-p38)/p-p65 signaling pathway and proinflammatory cytokines expression. *J Tradit Chin Med.* 2018;38(3):359–365.

Drug Design, Development and Therapy

Dovepress

Publish your work in this journal

Drug Design, Development and Therapy is an international, peer-reviewed open-access journal that spans the spectrum of drug design and development through to clinical applications. Clinical outcomes, patient safety, and programs for the development and effective, safe, and sustained use of medicines are a feature of the journal, which has also been accepted for indexing on PubMed Central. The manuscript management system is completely online and includes a very quick and fair peer-review system, which is all easy to use. Visit <http://www.dovepress.com/testimonials.php> to read real quotes from published authors.

Submit your manuscript here: <https://www.dovepress.com/drug-design-development-and-therapy-journal>